# DESIGN A NEW GENERATION OF 12% CHROMIUM STEELS

KME-710







**CONSORTIUM MATERIALS TECHNOLOGY** for thermal energy processes







# Design a new generation of 12% chromium steels

KME-710

FANG LIU AND HANS-OLOF ANDRÉN

# **Preface**

The project has been performed within the framework of the materials technology research programme KME, Consortium materials technology for thermal energy processes, period 2014-2018. The consortium is at the forefront of developing material technology to create maximum efficiency for energy conversion of renewable fuels and waste. KME has its sights firmly set on continuing to raise the efficiency of long-term sustainable energy as well as ensuring international industrial competitiveness.

KME was established 1997 and is a multi-cliental group of companies over the entire value chain, including stakeholders from the material producers, manufacturers of systems and components for energy conversion and energy industry (utilities), that are interested in materials technology research. In the current programme stage, eight industrial companies and 14 energy companies participate in the consortium. The consortium is managed by Energiforsk.

The programme shall contribute to increasing knowledge within materials technology and process technology development to forward the development of thermal energy processes for efficient utilisation of renewable fuels and waste in power and heat production. The KME goals are to bring about cost-effective materials solutions for improved fuel flexibility, improved operating flexibility, increased availability and power production with low environmental impact.

KME's activities are characterised by long term industry and demand driven research and constitutes an important part of the effort to promote the development of new energy technology with the aim to create value and an economic, environmentally friendly and long term sustainable energy society.

The industry has participated in the project through own investment (60 %) and the Swedish Energy Agency has financed the academic partners (40 %).

Bertil Wahlund, Energiforsk



## **Abstract**

Electricity generation from biomass will play an important role in the future. The main barriers to widespread use of biomass to generate electricity are cost and low energy efficiency, which is, in turn, limited by the materials. The proposed project aims to address the material challenges by using a new alloy design concept for 12% Cr steels -Z-phase strengthening. This is the only possible solution today to achieve both good creep and oxidation resistance for 12% Cr steels at 650°C. Based on our success in proving the novel concept of using Z-phase to strengthen 12% Cr steels from the previous KME project (KME 510), we continued our work on this new generation of martensitic steels. Within the frame of this project, we designed three new alloys. The aim was to understand the important factors that influence Z-phase formation, and thus aid the development Z-phase strengthened steels with high creep resistance. Firstly, we showed that Z-phase strengthened steels containing both Nb and Ta yield poorer creep strength compared to those containing only Ta. Secondly, a two-step tempering heat treatment procedure was optimized for all three test steels. Thirdly, we found carbon concentration was extremely important in the process of phase transformation to Z-phase; a high carbon concentration delayed the phase transformation. Therefore, we conclude a fine tune of the carbon concentration is essential in this type of steels. Finally, we found boron atoms segregated to prior austenite boundaries, lath boundaries, and the interface between Z-phase and steel matrix. The segregation likely plays an important role in lowering the interface energy, thus improving creep resistance.



# Sammanfattning

Den termiska verkningsgraden hos ångkraftverk begränsas av tillåten ångtemperatur och tryck, som i sin tur bestäms av korrosionsbeständigheten och kryphållfastheten hos tillgängliga stål. Alla försök hittills att överskrida 600-620°C med 11-12% kromstål har misslyckats, och vi förstår nu att anledningen är utskiljningen av en komplexnitrid, Z-fas, efter några års drift. Denna fas är grov och tillväxer på bekostnad av fina VN-utskiljningar, vilket leder till en dramatisk försämring av kryphållfastheten. Detta projekt syftar till att utveckla en ny generation martensitiska kromstål som använder Z-fas som härdande i stället för försvagande fas. De nya stålen har potentialen att användas i ångledningar och överhettare i framtida biobränsleeldade kraftverk med förhöjd driftstemperatur.

Det nära samarbetet mellan Chalmers tekniska högskola, Siemens Industrial Turbomachinery AB och Danmarks tekniska universitet har lett till att grundläggande kunskap vunnits om de nya Z-fasförstärkta stålen. Ett effektivt informationsutbyte inom den så väsentliga återkopplingen mellan legeringsdesign, mikrostrukturanalys och mekanisk provning har resulterat i en djup förståelse av systemet.

Baserade på idéprövningslegeringarna (proof-of-concept-legeringarna) som uppvisade utmärkt kryphållfasthet, i detta projekt finjusterade vi legeringssammansättningen för tre legeringar, och testade att kombinera Ta och Nb i Z-fas; och att öka kolhalt. Det visades sig att Ta baserade Z-fas ger bästa kryphållfasthet. Vid ökande kolhalt, sker fasomvandling mycket långsammare från MX till Z-fas. Vi utvecklade också mikrostrukturanalysmetoder för Z-fasförstärkta 12% kromstål.

Målet som uppsattes för projektet har framgångsrikt uppfyllts.

Nyckelord: 12% kromstål, Z-fasförstärkning, krypmotstånd, mikrostruktur



# **Summary**

The thermal efficiency of steam power plants is limited by the maximum allowed steam temperature and pressure, which in turn are determined by the corrosion and creep resistance of available steels. All attempts so far to exceed 600-620°C with 11-12% chromium steels have failed, and we now know that the reason is the precipitation of a complex nitride, Z-phase, after a few years of service. This phase is coarse and grows at the expense of fine VN precipitates, leading to a dramatic fall in creep strength. This project aims at developing a new generation of martensitic chromium steels that use Z-phase as a strengthening rather than weakening phase. The new steels have the potential to be used as piping or superheater tubing in future biomass power plants with increased operation temperature.

The close collaboration between Chalmers University of Technology, Siemens Industrial Turbomachinery AB, and the Technical University of Denmark has led to fundamental knowledge gained on the new Z-phase strengthened steels. The efficient exchange of information within the essential feedback loop between alloy designing, microstructure analyses, and mechanical testing have resulted in a deep understanding of the system.

Based on the success of the previous KME project in proving the concept of using Z-phase to strengthen 12% Cr steels, we further fine-tuned the chemical composition, designed and produced three test alloys, optimized heat treatment conditions for them. We addressed the following two issues: first, the effect of carbon addition; we found that carbon concentration is extremely important in the process of phase transformation to Z-phase. A high carbon concentration will delay the phase transformation. Second, steels with combining Ta- and Nb-containing Z-phase exhibit poor creep resistance. We also developed a toolbox of microstructure analysis methods for Z-phase strengthened 12% Cr steels.

The goal set for the project have been successfully fulfilled.

Keywords: 12%Cr steels, Z-phase strengthening, creep resistance, microstructure



# **List of content**

1	Intro	oduction	10
	1.1	Background	10
	1.2	Description of the research field	11
		1.2.1 Microstructure of conventional 9-12%Cr steels and	
		creep resistance	11
		1.2.2 Z-phase formation and strength breakdown	11
		1.2.3 New 12%Cr martensitic steels with Z-phase as strengthening precipitates	12
	1.3	Research task	12
	1.4	Goal	12
	1.5	Project organisation	13
		1.5.1 Industry reference and financing	13
		1.5.2 Staff 13	
		1.5.3 Project meetings	13
		1.5.4 Communication	14
2	Wor	k layout	16
3	Resu	ılts	17
	3.1	Alloy design	17
	3.2	Heat treatment optimization	17
	3.3	Mechanical testing	18
		3.3.1 Room temperature tensile, hardness and impact testing	18
		3.3.2 Long term creep testing	18
	3.4	Microstructure investigation	20
		3.4.1 Methodology development for microstructural analysis for Z-phase strengthened steels	20
		APT specimen preparation method for precipitates with low number density	20
		Possibility of using EFTEM for distinguishing Z-phase and Laves-phase	21
		APT for small precipitates in Z-phase strengthened steels	22
		3.4.2 Microstructure of trial steels	24
4	Ana	lysis of the results	35
	4.1	Inclusions and Primary Carbonitrides	35
	4.2	Secondary Precipitates	35



5	Conclusions	37
6	Goal fulfilment	38
7	Suggestions for future research work	39
8	Literature references	40
9	Publications	41
10	Appendices	42
	10.1 Experimental methods	42



# 1 Introduction

Design of a new generation of steels with significantly improved corrosion and creep resistance at  $650^{\circ}$ C promises increasing thermal efficiency in thermal power plants, and thus an improved efficiency in biomass fired plants, and even a potential annual saving in  $CO_2$  emissions from fossil-fired plants on an order of several gigatonnes globally. With the joint efforts of this project as well as other two closely related projects, we are aiming at designing and gaining understanding of a novel 12% chromium steel system – Z-phase strengthened steels.

#### 1.1 BACKGROUND

Biomass-fuelled power plants will contribute to provide a carbon neutral solution to Sweden's future energy security. However, the main barriers to widespread use of biomass for power generation are cost and low thermal efficiency, which in turn is largely limited by economically viable materials. Compared to the state of the art fossil-fired power plants, biomass fired power plants are run at a much lower temperature, due to severe corrosion attack to the fireside of the superheaters. For these power plants, focus is put on enhancing plant efficiency, mainly through increasing operating steam temperature and pressure. At the same time, we have to keep the construction and maintenance cost as low as possible, in order to make energy produced in these plants attractive to the energy consumers.

High temperature properties of the materials for the crucial components like superheaters in boilers set the limit on the possible improvement of efficiency in these plants. The materials must be capable of being operated at high temperatures and stresses for prolonged time. Hence, degradation mainly due to creep and corrosion must be minimized. For biomass fired power plants, the nearest goal is to increase the steam temperature to 600°C, which means that the temperature of the metal in the superheater is around 630-650°C. Tempered martensitic 9–12% chromium steels offer an optimal combination of the critical properties, i.e. creep strength, corrosion resistance at the steam-side, at a relatively low cost. Therefore, with a proper coating at the fireside, a new generation of 9–12% chromium steels, which possesses high creep strength and steam corrosion resistance at 650°C, can provide reliable and relatively cheap superheaters for the biomass fired power plants.

If we look at the problem on a global level, fossil fired power plants provide more than 70% of the world's electricity and account for about one third of global CO<sub>2</sub> emissions, which reached an all-time high of 35 gigatonnes (Gt) in 2015 [1, 2]. A transition from fossil power plants to renewable energy sources is desirable from an environmental point of view. Combustion of biomass has shown great potential to combat CO<sub>2</sub> emission. This process is often considered "zero emission", since the biomass has to bind up CO<sub>2</sub> during the growth.

In this project we performed systematic research in order to gain a comprehensive understanding on the mechanical properties in particular creep properties of these steels, and we provided fundamentally important knowledge, which has been fed into the improvement of the new steels.



#### 1.2 DESCRIPTION OF THE RESEARCH FIELD

## 1.2.1 Microstructure of conventional 9-12%Cr steels and creep resistance

Tempered martensitic steels are usually austenitized at ~ 1100°C followed by tempering heat treatment. They exhibit a typical microstructure, which consists of prior austenite grain boundaries, blocks, laths, high density of dislocations and precipitates. In the technically interesting stress and temperature range for these steels, the main creep mechanism is dislocation creep. Therefore, the ways to retard or delay dislocation glide and climb are helpful to improve creep resistance [3]. The most important strengthening mechanism is precipitation hardening [4].

The size and number density of the precipitates at the initial stage, as well as their stability against coarsening during exposure to high temperatures play a vital role in creep. The most important precipitates are carbide  $M_{23}C_6$  (M = Fe, Cr, Mo), nitride MN (M = V, Nb, Cr) [4], intermetallic Laves phase Fe<sub>2</sub>M (M = Mo, W), and complex nitride Z-phase (Cr,Fe)MN (M = V, Nb, Ta).

M<sub>25</sub>C<sub>6</sub> precipitates are the major strengthening particles for the first generation of 9-12%Cr steels like X20CrMoV121. They are mainly located at the prior austenite grain boundaries and lath boundaries, with a typical size of 100 nm after tempering and a few hundred nanometres after prolonged exposure. At late 1970's, researchers at Oak Ridge National Laboratory succeeded in obtaining very fine distributed MN precipitates by adding very small amount of V or Nb and N into the famous alloy – ASTM grade P91. And a few years later, another commercial steel ASTM grade P92, which has similar chemical composition as P91 but adding W and B, was launched. P91 and P92 are mainly based on particle strengthening with MN and M<sub>23</sub>C<sub>6</sub>. Compared to M<sub>23</sub>C<sub>6</sub>, MN has a much smaller particle size, usually at the range of 20 nm after tempering, and higher number density and more significantly they are very stable against coarsening in P91 and P92 [5]. This makes P92 two times as strong as the old X20CrMoV121 at 600°C.

Laves phase may form in Mo or W containing steels. It has a long nucleation and growth phase at 600°C. W containing Laves phase nucleates faster, thus leading to finer and more densely distributed precipitates.

#### 1.2.2 Z-phase formation and strength breakdown

P92 contains only 9 wt.% Cr, which is too low in terms of corrosion resistance at 650°C. It has been established that at high temperatures the corrosion resistance of a steel is proportional to its Cr content; the higher the Cr content, the better the corrosion resistance [6]. Therefore, there have been several recent trials aiming for improving both creep and corrosion properties by adding e.g. Co, W and B to the steels, in combination with a higher Cr content (11-12% vs. 9% in P92). Nevertheless, all of them turned out to be failures. Although they showed better creep resistance at 650°C than older steels until ~10,000 hours, they then suffered a dramatic loss of creep strength [7].

There was debate on the mechanisms behind the dramatic breakdown. Now it is widely accepted that this is mainly attributed to the precipitation of a complex nitride known as



Z-phase ((Cr,Fe)(Nb,V) N) during creep. Many small MN precipitates are dissolved to form large Z-phase particles, which are thermodynamically more stable at this temperature but give very little contribution to creep strength [8, 9]. Z-phase formation in a number of 9-12%Cr steels, which rely mainly on MN for strengthening, has been systematically studied. It has been shown that a Cr content above 10.5% strongly accelerates Z-phase formation. In contrast steels with 9% Cr or below are largely unaffected by the Z-phase precipitation up to 100,000 hours at 600-650°C [10].

#### 1.2.3 New 12%Cr martensitic steels with Z-phase as strengthening precipitates

Z-phase precipitates were credited as beneficial for strengthening in creep resistant austenitic steels containing Nb, since they precipitate quickly among the first appearing precipitates and as fine densely distributed particles [11].

Our collaborator Prof. Hald and co-workers from the Technical University of Demark proposed a new alloy design concept, which makes use of Z-phase as strengthening dispersion for 9-12%Cr martensitic steels, instead of MN. The new steels are supposed to be strengthened by fine Z-phase precipitates, which are formed during heat treatment or at the early stage of application. Good creep resistance would be expected, if densely distributed fine Z-phase precipitates can be formed during heat treatment and if they coarsen slowly during service.

#### 1.3 RESEARCH TASK

Our task was to develop new 12% chromium steels for up to 650°C, by studying the microstructure and mechanical behaviour of Z-phase strengthened alloys. The work was to be performed by high-resolution microscopy and microanalysis (scanning electron microscopy (SEM), transmission electron microscopy (TEM), and atom probe tomography (APT)) at Chalmers, Göteborg, and heat treatment, mechanical and creep testing at Siemens, Finspång.

Within the frame of this project we planned to:

- design three new test steels with fine-tuned chemical composition, aiming for improved creep resistance compared to the ones that have been designed and investigated in the previous KME 510 project;
- Optimize heat treatment conditions for test steels;
- Perform mechanical and creep testing on promising test steels with optimized heat treatment;
- Understand the sophisticated effects of carbon addition on the precipitation reaction sequences in the Z-phase strengthened steels;
- Understand effects of small addition of B on the Z-phase strengthened steels;

#### 1.4 GOAL

The long term goal of this project was to provide fundamentally important knowledge on the sophisticated process-microstructure-properties relationships, which can be fed into the improvement of the new steels so that the new steels with optimal combination



of corrosion and mechanical properties can be exploited for use in bio-mass fuelled thermal power plants.

#### 1.5 PROJECT ORGANISATION

#### 1.5.1 Industry reference and financing

Siemens Industrial Turbomachinery AB (Lennart Johansson) participated in the project, and performed in-kind work (tensile testing, impact toughness testing, creep testing, reporting and travel) at a planned cost of 1,200,000 SEK during 2014-2018.

Additional financing was received from the Research Foundation of VGB (2015-2018), EU project European FP7 cooperation project on Z-phase steels – Z-Ultra (2013-2016).

#### 1.5.2 Staff

At Chalmers University of Technology, Associate Professor Fang Liu worked 10%, Emeritus Professor Hans-Olof Andrén worked 10%, and Ph.D student Masoud Rashidi (received his PhD degree on 1st Dec. 2017) worked 90% in this project. Fang Liu was on maternity leave from November 2014 to June 2015, Prof. Andrén acted as the project leader during her absence.

At Technical University of Denmark (DTU), Prof. John Hald, postdoctoral researcher Chitta Ranjan Das, PhD student Irina Fedorova, participated in the project.

At Siemens Industrial Turbomachinery AB, Finspång, Sweden, Lennart Johansson, and at Siemens, Mülheim, Germany, Dr. Torsten Kern participated in the project.

#### 1.5.3 Project meetings

Regular project meetings have been held through the project period. Every 4 months project participants attend the meeting. Chalmers, DTU and Siemens host the meetings in turn. During the meeting, results from all parties were presented, and a work plan was agreed by all parties. A brief of all project meetings are listed below.

- The first project meeting was hold at Siemens, Finspång, on 4th December 2014. Participants: Hans-Olof Andrén, Masoud Rashidi, John Hald, Torsten Kern, Arne Karlsson, and Lennart Johansson.
- The second project meeting was hold at DTU, Denmark, on 9th April 2015. Participants: Hans-Olof Andrén, Masoud Rashidi, John Hald, Frank Niessen, Torsten Kern, and Lennart Johansson
- **The third project meeting** was hold at Chalmers University of Technology, Gothenburg, on 3rd September, 2015.

Participants: Fang Liu, Hans-Olof Andrén, John Hald, Chitta Ranjan Das and Irina Fedorova, Torsten Kern, and Lennart Johansson.



- The fourth project meeting was at Siemens, Finspång, on 17<sup>th</sup> December 2015. Participants: Fang Liu, Hans-Olof Andrén, Chitta Ranjan Das, Irina Fedorova, Torsten Kern, and Lennart Johansson.
- The fifth project meeting was hold at DTU, Denmark, on 14th April 2016. Participants: Fang Liu, Hans-Olof Andrén, Masoud Rashidi, Robert Lawitzki (Master's student), John Hald, Kristian Vinter Dahl, Chitta Ranjan Das, Irina Fedorova, Torsten Kern, and Lennart Johansson.
- The sixth project meeting was hold at Chalmers University of Technology, Gothenburg, on 13th September 2016.

  Participants: Fang Liu, Hans-Olof Andrén, Masoud Rashidi, John Hald, Chitta Ranjan Das, Irina Fedorova, Torsten Kern, and Lennart Johansson.
- The seventh project meeting was hold at Siemens, Finspång, on 8th December 2016. Participants: Fang Liu, Hans-Olof Andrén, Masoud Rashidi, John Hald, Chitta Ranjan Das, Irina Fedorova, Torsten Kern, and Lennart Johansson.
- The eighth project meeting was hold at Chalmers University of Technology, Gothenburg, on 20th March 2017.

  Participants: Fang Liu, Hans-Olof Andrén, Masoud Rashidi, John Hald, Torsten Kern, and Lennart Johansson.
- The ninth project meeting was hold at DTU, Denmark, on 6th September 2017. Participants: Fang Liu, Hans-Olof Andrén, John Hald, Torsten Kern, and Lennart Johansson.
- The tenth project meeting was hold at Siemens, Finspång, on 19th December 2017. Participants: Fang Liu, Hans-Olof Andrén, John Hald, Irina Fedorova, Eva Oscarsson, Torsten Kern, Kim Färnlund, and Lennart Johansson attended the meeting.
- The eleventh project meeting was hold at Chalmers University of Technology, Gothenburg, on 15th March, 2018.

  Participants: Fang Liu, Hans-Olof Andrén, Masoud Rashidi (on invitation), John Hald, Irina Fedorova, Torsten Kern (via net meeting), and Lennart Johansson.

#### 1.5.4 Communication

A web-based communication tool has been set up. Minutes and presentations from all the project meetings are available for all participants on the internal website.

Results from the project have been presented in four articles in peer reviewed international journals, and four international conferences.

- A new 12% chromium steel strengthened by Z-phase precipitates
   F. Liu, M. Rashidi, L. Johansson, J. Hald, H.-O. Andrén Scripta Materialia, Vol. 113, 93-96, 2016.
- Microstructure of Z-phase strengthened martensitic steels: meeting the 650°C challenge
   F. Liu, M. Rashidi, J. Hald, L. Reißig, and H.-O. Andrén
   Materials Science Forum, Vol. 879, 1147-1152, 2016.



 Core-Shell Structure of Intermediate Precipitates in a Nb-Based Z-Phase Strengthened 12% Cr Steel

M. Rashidi, H.-O. Andrén, F. Liu *Microscopy and Microanalysis*, Vol. 23, 360-365, 2017.

- Microstructure and mechanical properties of two Z-phase strengthened 12% Cr martensitic steels: the effects of Cu and C
   M. Rashidi, L. Johansson, H.-O. Andrén, F. Liu
   Materials Science and Engineering A, 694, 57-65, 2017.
- Microstructure characterization of two Z-phase strengthened 12% chromium steels
  M. Rashidi, F. Liu and H.-O.Andrén
  10th Liège Conference on Materials for Advanced Power Engineering. September 14th 17th,
  2014.
- Tantalum and niobium based Z-phase in a Z-phase strengthened 12% Cr steel
  M. Rashidi, R. Lawitzki, H.-O. Andrén, and F. Liu
  EPRI 8th International Conference on Advances in Material Technology for Fossil Power
  Plants, October 11 -14, 2016.
- On the non-equilibrium segregation of Boron in 9-12%Cr steels
   I. Fedorova, F. B. Grumsen, F. Liu, J. Hald
   4th International ECCC Creep & Fracture Conference, September 10-14, 2017, Düsseldorf, Germany.
- Role of copper on Laves phase morphology in 9-12%Cr steels
   H. K. Danielsen, F. Liu
   IOP Conference Series: Materials Science and Engineering, Volume 219. 38th Riso
   International Symposium on Materials Science, Riso, Denmark, 4-8 September 2017. IOP Conf. Ser.: Mater. Sci. Eng. 219, 012015



# 2 Work layout

Chalmers was responsible to analyze the microstructure of the test steels using advanced microstructure and microanalysis techniques: SEM, TEM and APT; to establish the relationships between the steels' chemical composition and heat treatment, microstructure, and properties, in particular on the formation of precipitates, and also coordinated the project.

Siemens was responsible to perform heat treatment, and mechanical testing, including tensile testing, long-term creep testing, hardness testing, and impact toughness testing.

DTU was responsible to provide the testing alloys, and establish the relationships between the steels' chemical composition and heat treatment, microstructure, and properties, in particular on the formation of reverse austenite using X-ray radiation, and the nature of boron segregation.

There is a loop of information flow between the project partners, and all obtained information on the microstructure was used to improve the alloy design.



# 3 Results

#### 3.1 ALLOY DESIGN

Alloy design was guided by modelling (performed mainly by DTU) in combination with a continuously deepened understanding of the relationships between mechanical properties (tested mainly by Siemens) and the microstructure (investigated mainly by Chalmers) of this new alloy system. The chemical compositions of the three alloys are listed in Table 1. We mainly studied three aspects of the alloys: 1) the effect of combination of Ta and Nb (ZU2); 2) the effect of carbon concentration (ZU3); 3) the effect of adding Mo.

**Table 3-1.** Nominal composition of the test Z-strengthened steels ZU1, ZU2, and ZU3 (in **atomic** percent, and Fe in balance).

Steel	Ni	Со	Cr	W	Nb	Ta	Cu	Mo	C	В	N	Si	Mn
ZU1	0.17	2.66	12.10	0.61	-	0.10	1.76	-	0.13	0.02	0.18	0.68	0.12
ZU2	0.16	3.10	12.10	0.64	0.10	0.06	1.90	0.13	0.14	0.03	0.17	0.64	0.13
ZU3	0.20	2.95	11.9	0.54	-	0.13	-	0.29	0.23	0.02	0.14	0.45	0.12

## 3.2 HEAT TREATMENT OPTIMIZATION

For 9-12%Cr steels heat treatment plays an important role in dictating their creep properties. The typical heat treatment procedures are:

- Austenitization (sometimes also called normalization) at > 1000°C;
- Quenching, usually in air, to obtain a martensitic structure with supersaturated carbon. At this stage the steel has very high strength, but is too brittle to be used.
- Tempering at 700-800°C. At this stage precipitation of nano-sized strengthening particles takes place. The hardness of the steel decreases dramatically.

The aim is, by performing systematic investigation, to provide a guideline of heat treatment for the new martensitic steels. This practical guideline ensures an optimal combination of strength, ductility, and toughness.

Based on our previous experience on 9-12%Cr steels, the heat treatment conditions for the alloys was designed to be: austenitization temperature at  $1100^{\circ}$ C, and then a two-stage tempering:  $650^{\circ}$ C 4 h +  $750^{\circ}$ C 2 h.

We chose a relatively high austenitization temperature 1100°C in between 1150°C and 1050°C. This is a comprise between industry practice (a temperature higher 1100°C is very difficult to achieve) and scientific understanding (to dissolve as many primary TaC as possible, and make more Ta available for forming Z-phase in subsequent heat treatment). During the two-stage tempering, the first stage allows part of the Cu to precipitate out of the ferrite matrix, and this will increase the A<sub>1</sub> temperature of the



remaining steel matrix. With an increased  $A_1$  temperature, the second stage tempering can be carried out at a higher temperature.

#### 3.3 MECHANICAL TESTING

For future applications, besides good long-term mechanical properties and corrosion resistance at elevated temperatures, all the test alloys must possess reasonable mechanical properties at room temperature.

#### 3.3.1 Room temperature tensile, hardness and impact testing

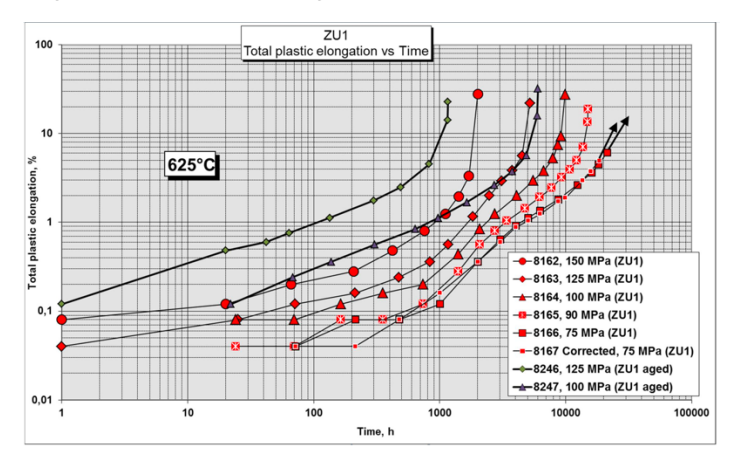
Tensile, hardness and impact testing were performed on ZU1, ZU2, and ZU3 samples that were austenitized at  $1100^{\circ}$ C and then tempered at  $650^{\circ}$ C 4 h +  $750^{\circ}$ C 2 h. The results are shown in *Table 2*.

Table 2. Tensile, hardness and impact testing results for the test alloys.

Material	Rp (MPa)	Rm (MPa)	A5 (%)	Z (%)	Hard ness	KV (J)
ZU1	699	802	18.5	71.1	262	198
ZU2	670	774	19.4	71.5	253	149
ZU3	658	779	19.6	76.2	252	205

## 3.3.2 Long term creep testing

Creep rupture testing at  $625^{\circ}$ C for ZU1, ZU2, and ZU3 ( $1100^{\circ}$ C/1h +  $650^{\circ}$ C/4h +  $750^{\circ}$ C/2h) was performed by Siemens. The results are shown in Figure 1 a), b), c) and d), respectively. A few testing of ZU1 and ZU4 at certain stress levels is still under progress (the data points with an arrow in Figure 1). The creep rupture results, obtained so far, in comparison with ZL3, the alloy from previous project, KME 510, with optimized creep and impact toughness, are shown in Figure 2.



a)



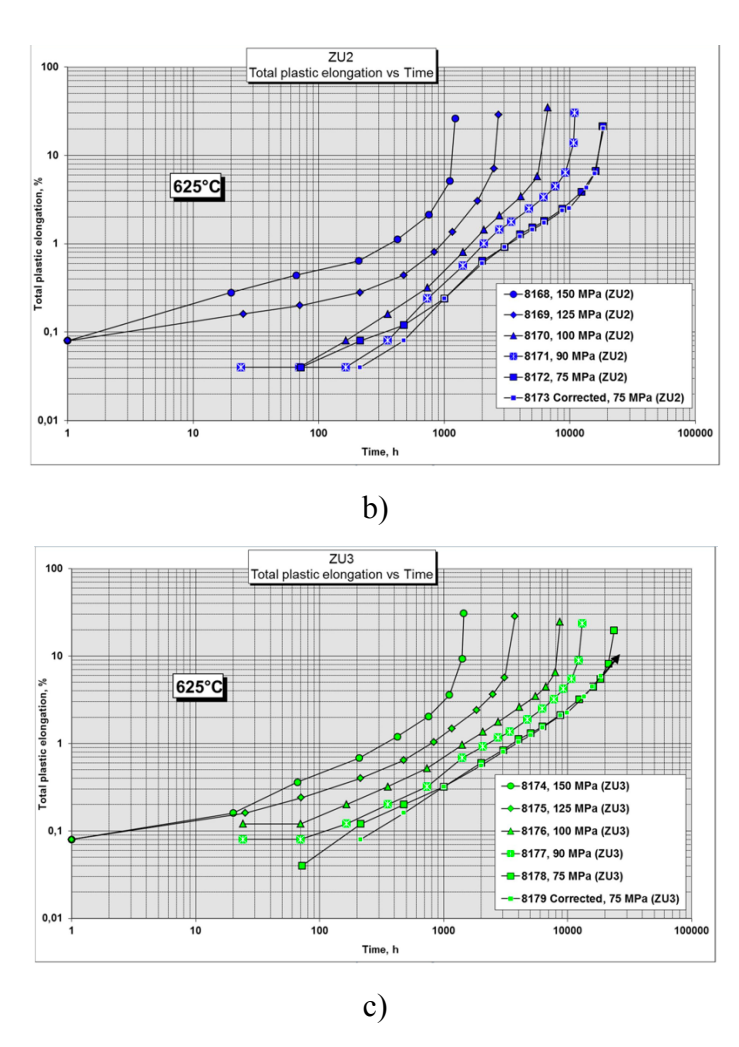


**Figure 1.** Creep elongation curves at  $625^{\circ}$ C for a) ZU1, b) ZU2, and c) ZU3 (austenitization 1100 °C for 1 h, tempering  $650^{\circ}$ C 4h +  $750^{\circ}$ C for 2 h).

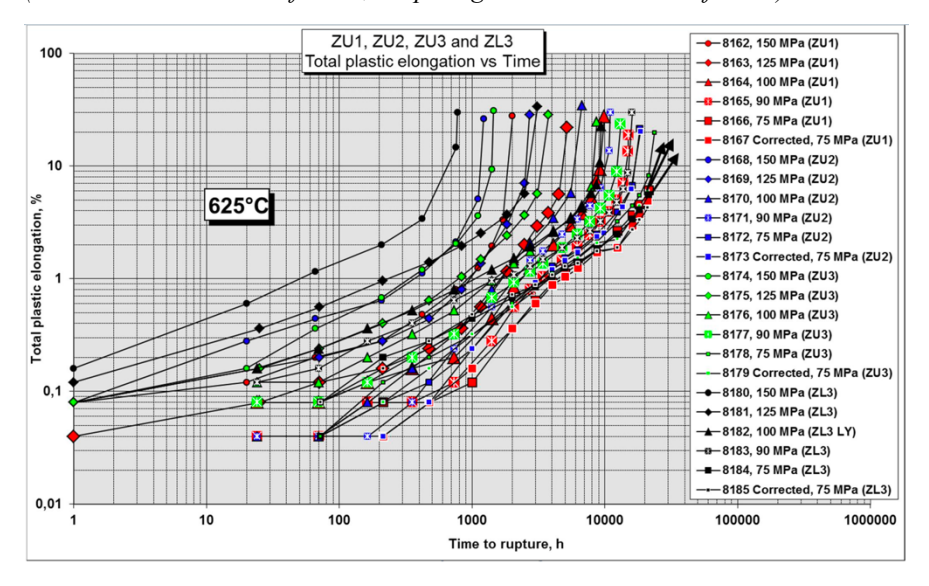


Figure 2. Creep elongation curves of ZU1, ZU2, and ZU3 in comparison with ZL3 (in black), a test alloy from previous project.



#### 3.4 MICROSTRUCTURE INVESTIGATION

Microstructure dictates properties of materials. For this new generation of steels, a systematic investigation of their microstructure, and microstructure evolution at high temperatures is essential to understand their mechanical behaviour. And in turn the understanding gained on microstructure facilitates further alloy design optimization, which can lead to improved mechanical properties. Advanced microstructural analysis techniques, such as scanning electron microscopy (SEM), transmission electron microscopy (TEM), and atom probe tomography (APT) were used.

This section is organized like this: first we show the results of the microstructure analysis methodological development performed within this project: sample preparation optimization and high resolution backscattered electron imaging in SEM; then we present the detailed microstructure study results of different test alloys.

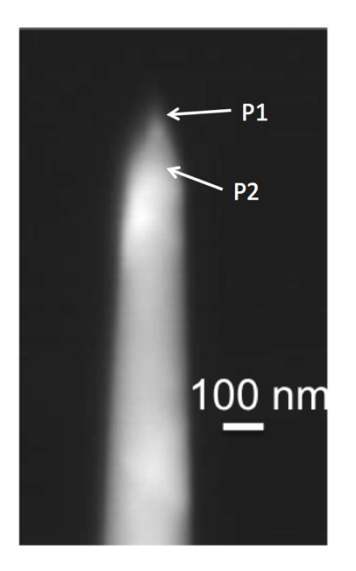
3.4.1 Methodology development for microstructural analysis for Z-phase strengthened steels

#### APT specimen preparation method for precipitates with low number density

In most of the cases, we used the two-stage electropolishing method to prepare needle-shaped atom probe tomography (APT) specimens. The advantages of this method are i) the experimental equipment is relatively simple, ii) the throughput is high. This method is powerful for analysing precipitates with high number density, such as Z-phase precipitates in as-tempered condition or after short aging time. For analysing precipitates with a low number density, such as Z-phase precipitates after a long aging time or Lavesphase precipitates, it often requires analysing a large number of specimens, if we only use random specimens prepared by the two-stage method. To tackle this problem, previously researchers performed the so-called back polishing – they removed a small volume of the APT specimen at a time using electropolishing in a diluted electrolyte, and then observed the specimen under a TEM. They repeat this procedure until they obtained a targeted precipitate. However, this method is rather time consuming, and the process cannot be precisely controlled.

To obtain targeted precipitates, instead of the back-polishing method we make use of a combined focused ion beam and SEM instrument, a FIB/SEM. Thanks to the capability of live time imaging of the specimen enabled by the SEM part, this instrument allows precisely controlled ion milling using the FIB part. Since both Z-phase and Laves-phase precipitates contain heavy elements, i.e. Ta and W, they are readily observable in the SEM. Using this method, we successfully prepared APT specimens containing Z-phase and Laves-phase (Figure 3) precipitates.





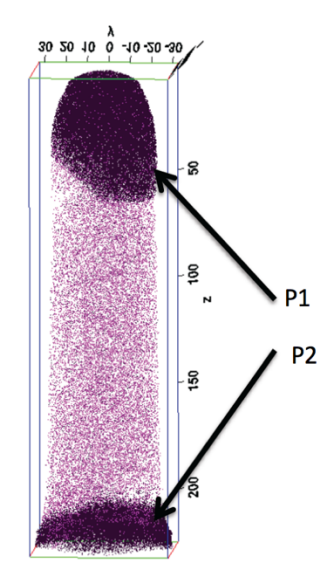


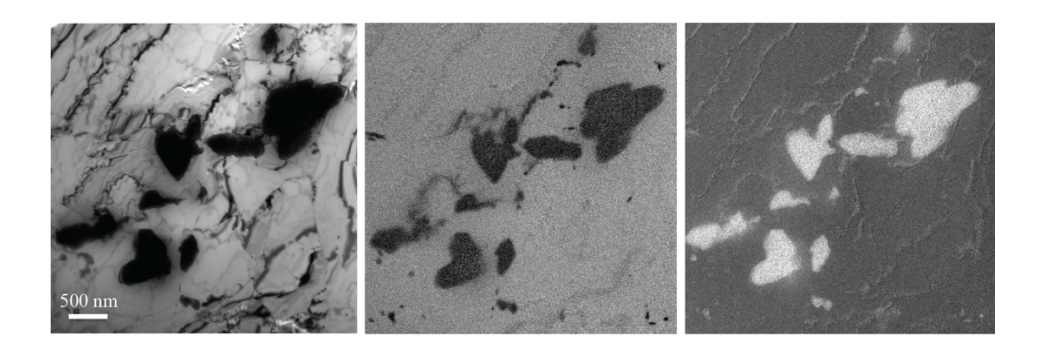
**Figure 3.** (a) SEM micrograph of an APT specimen tip (by FIB/SEM). The bright contrast of the Laves-phase precipitates enables us to precisely locate these precipitates. (b) APT reconstruction of the same specimen. Both Laves-phase precipitates were analysed by APT.

## Possibility of using EFTEM for distinguishing Z-phase and Laves-phase

Energy filtered transmission electron microscopy (EFTEM) has been exploited to study small precipitates in 9-12% Cr steels, such as M<sub>23</sub>C<sub>6</sub> and MX. Different families of precipitates are nicely revealed, using normally Fe, Cr and V signals, which give elemental maps with good quality. Compared to bright field imaging, EFTEM is considered very powerful, especially in revealing the extremely small precipitates, such as MX. This is because in a bright field image the contrast yielded by the tiny MX precipitates is very weak, while other contrast yielded by bending fringes, dislocations, and diffraction are remarkably stronger, and thus making unambiguous quantitative analysis of the precipitates impossible (see Figure 4). This was the initial motivation of using EFTEM to quantify Z-phase.

However, in the Z-phase strengthened steels using EFTEM to identify Z-phase was found challenging. The continuous transformation from MX to Z-phase and varying amount of Cr in these particles, make it difficult to distinguish between Z-phase and a partially transformed MX to Z-phase. Besides, Z-phase contains mainly Cr, Ta and N, and Laves-phase contains mainly Fe, W and substantial amount of Cr. Since the Fe concentration in Z-phase and Laves-phase is significantly lower than that in the matrix, both Z-phase and Laves-phase yield dark contrast in the Fe map (Figure 4). Since the Cr concentration in Z-phase and Laves-phase are rather high (~ 17% in Laves-phase), both families of precipitates yield bright contrast in the Cr map (Figure 1-3). Although even very small precipitates are nicely revealed in both Fe and Cr maps, Laves-phase and Z-phase precipitates cannot be distinguished. In addition, W and Ta signals are weak and located closely, thus they are not ideal to be used to produce EFTEM images. N signals are also weak compared to the background. Therefore, EFTEM was not used to distinguish different families of precipitates.





Bright field image Fe map Cr map

**Figure 4.** EFTEM bright field image, Fe map and Cr map. Note that the small precipitates are visible, however, Z-phase cannot be distinguished from Laves-phase.

#### APT for small precipitates in Z-phase strengthened steels

Energy Dispersive X-ray Spectroscopy (EDS) in TEM is quite limited in determining the composition of small precipitates that contain light elements such as N and C. APT detecting all elements with equal sensitivity provides the possibility of analysing carbides and nitrides in 9-12% Cr steels in more detail. However, these precipitates have mostly high evaporation field compared to the steel matrix. Hence, local magnification and trajectory aberration artefacts can complicate obtaining an accurate chemical composition and morphology of these small precipitates. We developed a method to accurately measure the composition of small precipitates that suffer from local magnification artefacts using APT.

Three possible ways to analyse these small precipitates using IVAS<sup>TM</sup> software are compared: 1D concentration profiles, proxigrams, and iso-concentration surfaces. A 1D concentration profile across a precipitate and a proxigram (Figures 5 a, and b) provide important information on the distribution of the elements. For example, it is shown that the precipitate is depleted in Fe and contains Cr, N, and Nb. However, one must be very careful interpreting the obtained results due to the peak overlaps between different ions, for example Fe<sup>2+</sup> and N<sup>2+</sup>, Si<sup>2+</sup> and N<sup>+</sup>, and Fe<sup>2+</sup> and Cr<sup>2+</sup>. In addition, the obtained data are disturbed due to the local magnification effect, and consequently the contribution from the matrix.

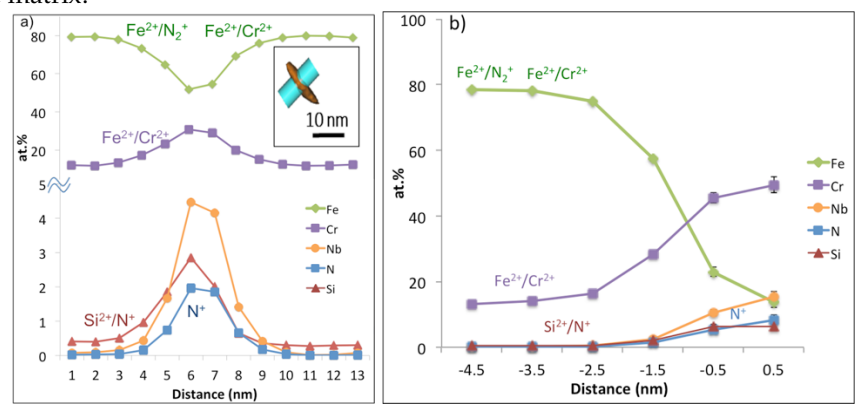


**Figure 5.** a) 1D concentration profile across a blade-like precipitate. Inset shows the position of the cylinder in relation to the precipitate. b) Proxigram using the IVAS software.



In order to solve the issue with peak overlaps, one can extract the ions belonging to the precipitate using iso-concentration surfaces and use the built-in peak deconvolution tool in IVAS<sup>TM</sup>. Normally, the iso-concentration value is selected in a way that the least contribution from matrix is involved. However, by doing this a lot of ions belonging to the precipitate are not measured and the composition of the core of the particle is considered as the composition of the whole particle.

Thus, in order to accurately measure the composition of these small precipitates, the following routine was employed. First of all, the matrix composition was accurately measured in volumes where neither precipitates nor grain boundaries existed. Then, the composition of the precipitates with low iso-concentration values was collected in order to include as many ions belonging to the precipitate into the composition as possible. This procedure obviously led to measuring the precipitate plus matrix composition (Table 3). At this point using the built-in peak deconvolution tool in IVAS<sup>TM</sup>, the mentioned peak overlaps are solved. By considering the fact that there is almost no Co in Z-phase, one can deduct the Co content and proportionally other alloying elements in the matrix from the precipitate plus matrix composition. The remaining atoms belong to the precipitate. Hence, the composition of the precipitate can then be obtained.

	Matr	ix	Matrix+	particle	Cori	rection base	d on removi	ng Co	Correction based on removing Fe			
Elements	Counts	%	Counts	%	$\begin{array}{c} Co_{PM}/\\ Co_{M} \end{array}$	Expected Matrix	PM-EM (particle)	Particle (at.%)	Fe <sub>PM</sub> / Fe <sub>M</sub>	Expected Matrix	PM-EM (particle)	Particle (at.%)
Cr	2431673	12.30	60411	26.05	0.0032	7782	52629	31.20	0.0034	8221	52190	31.61
N	3697	0.02	52839	22.78		12	52827	31.32		12	52827	32.00
Fe	15860080	80.26	53622	23.12		50757	2865	1.70		53622	0	0
Nb	75	0	51175	22.07		0	51175	30.34		0	51175	31.00
W	34836	0.18	2231	0.96		111	2120	1.26		117	2114	1.28
Co	1038645	5.26	3324	1.43		3324	0	0		3511	-187	-0.11
V	672	0	1672	0.72		2	1670	0.99		2	1670	1.01
В	244	0	1387	0.60		1	1386	0.82		1	1386	0.84
C	163	0	2448	1.06		1	2447	1.45		1	2447	1.48
Mn	83254	0.42	690	0.30		266	424	0.25		281	409	0.25
Ta	0	0	212	0.09		0	212	0.13		0	212	0.13
Ni	195529	0.99	1343	0.58		626	717	0.43		661	682	0.41
Si	113105	0.57	549	0.24		362	187	0.11		382	167	0.10

In case of very small precipitates, the number of Co atoms is low and consequently big errors could be introduced to the composition. Thus, one can deduct the matrix composition based on the "Fe correction" meaning that the Fe and proportionally other elements are removed from the precipitate plus matrix composition. By considering the fact that Z-phase can dissolve 1-3 at.% Fe, a small systematic error to the composition was introduced. The minus value for the Co content in the "Fe correction" method is due to the small solubility of Fe in Z-phase. Yet, as can be seen in Table 3, there is a good agreement between the compositions obtained by "Co correction" and "Fe correction".



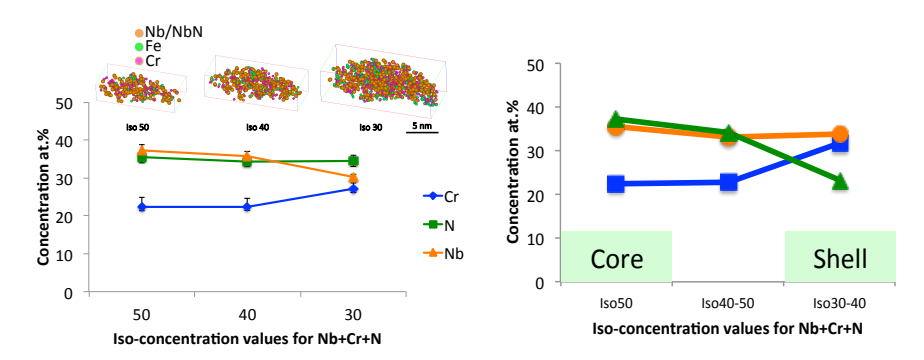


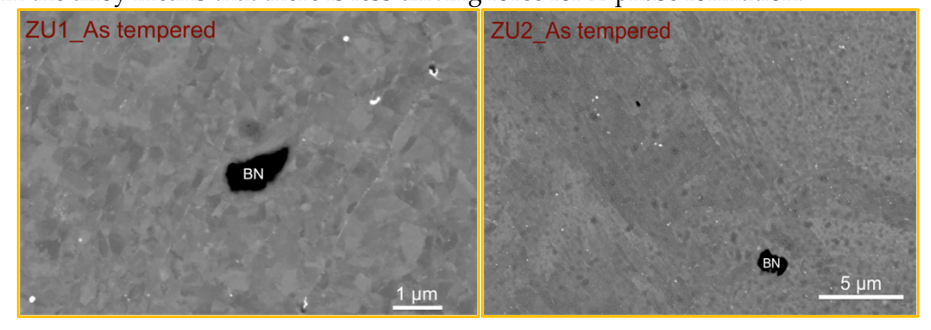
**Figure 6.** The composition of a Nb-containing Z-phase precipitate a) based on Fe-correction and iso-surface; b) based on Fe-correction and the concentration difference between iso-surfaces, i.e. concentration of different layers.

In Figure 6, the composition of a precipitate obtained from "Fe correction" routine is presented for the trial steel aged for 24 hours at 650°C. As can be seen, the composition varies slightly between the iso-concentration surface value of 50 and 30. Iso 50 shows the composition of the core of the precipitate, while iso 30 contains both core and shell of the precipitate. The graph shows that the Cr concentration in the shell of the precipitate is higher compared to the core of the precipitates. By deducting the obtained composition of different iso-surfaces, we can measure the composition of different layers of the precipitate. Figure 6 b) shows the composition of the precipitates layer by layer in the precipitate.

#### 3.4.2 Microstructure of trial steels

## Primary particles

As can be seen in Figure 7, in ZU1, ZU2 and ZU3 series trial steels BN particles were formed. These BN particles consume beneficial elements B and N. B is believed to decrease the coarsening rate of  $M_{23}C_6$  and MX particles. The decreased N concentration in the alloy means that there is less driving force for Z-phase formation.





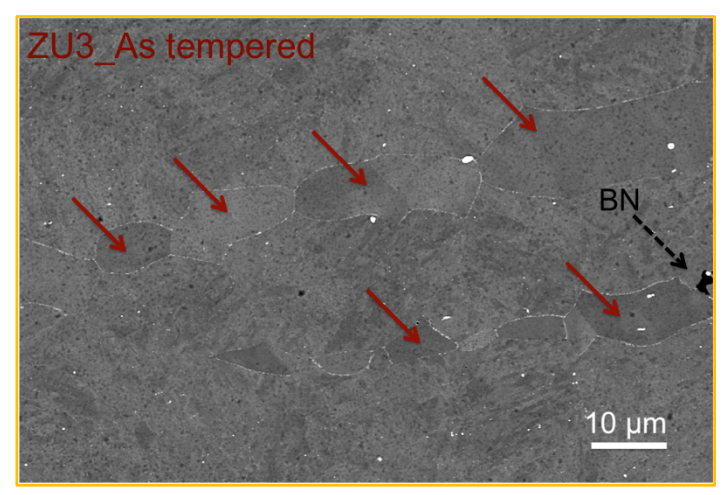


**Figure** 7. SEM micrographs showing BN particles in ZU1, ZU2, and ZU3. In ZU3 alloy, red solid arrows showing  $\delta$ -ferrite grains.

Figures 8 – 10 show primary MX particles in the ZU1, ZU2 and ZU3 series steels. These particles mainly contain Ta, Nb, C, and N. Primary MX particles are desired as they can lock the prior austenite grain boundaries and control grain coarsening during the austenitization process. These particles consume C, thus there is less C left in the steel. It has been found in the ZL3 steel that C can react with Ta to form Ta(C,N), which may delay the transformation to Z-phase CrTaN, compared with pure TaN. Therefore, less available C in the steel can accelerate the transformation to Z-phase. However, these primary particles also consume elements that are needed to form Z-phase, such as Ta, Nb and N.

In ZU1, primary particles are mainly TaC. These are shown by arrows in Figure 8 with a typical EDX spectrum for these particles. The Fe signal comes from the steel matrix.

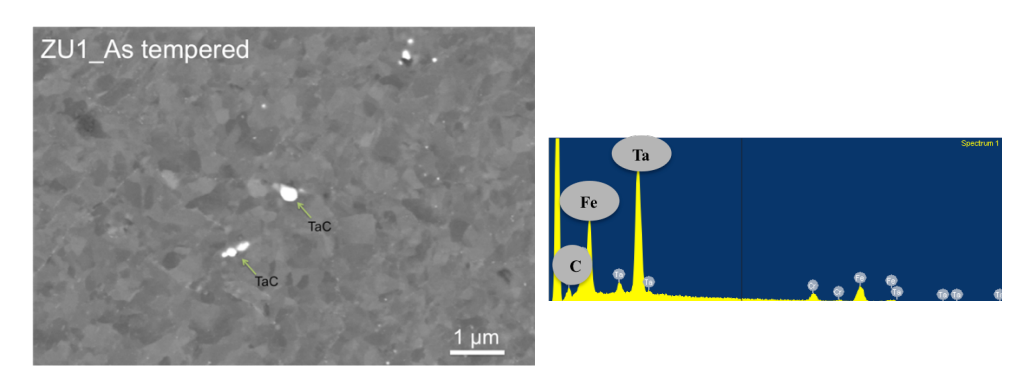


**Figure 8**. SEM micrograph of ZU1 as-tempered showing TaC particles and a typical EDX spectrum for these particles.

In ZU2 steel, adding Nb to the system resulted in primary (Ta,Nb)(C,N,B) particles, see Figure 9. Previously, we have not observed particles with high carbon, nitrogen and boron contents – usually either carbonitrides or borocarbides are formed. In fact, these primary particles in ZU2 alloy consume more beneficial elements such as N and B compared to the primary particles in other trial steels. This behaviour will probably result in less Z-phase formation (due to less available N in the matrix) and higher coarsening rate for  $M_{23}C_6$ , and secondary MX particles due to less B content (B is believed to control the coarsening rate of  $M_{23}C_6$  and secondary MX particles).



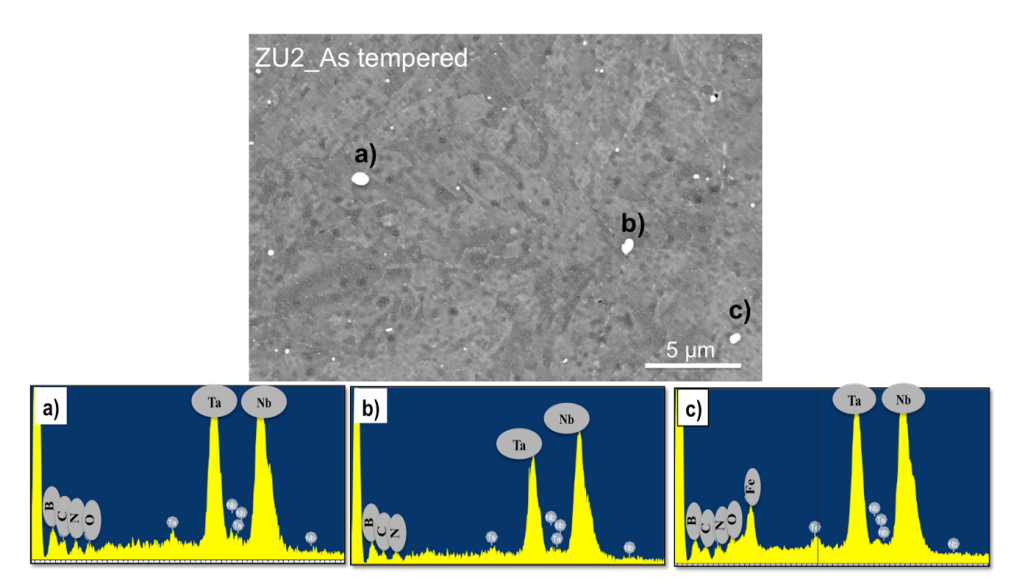


**Figure 9**. SEM micrograph of ZU2 as-tempered showing primary (Ta,Nb)(C,N,B) particles and corresponding EDX spectra for these particles.

Primary MX particles in ZU3 trial steel are mainly TaC, see Figure 10.

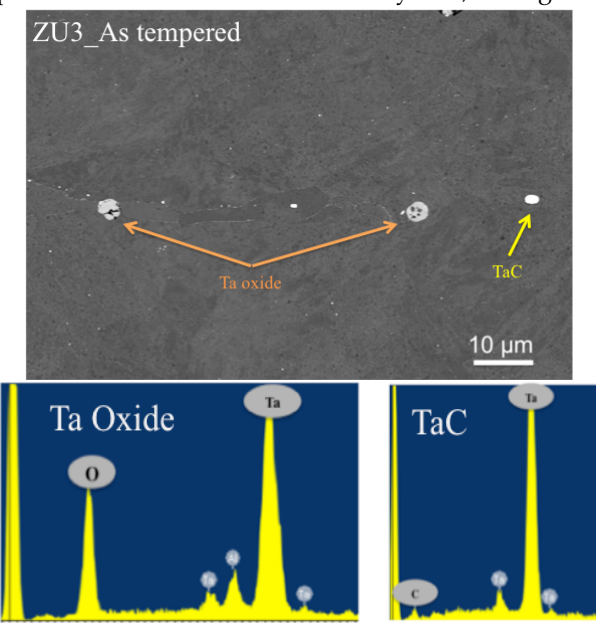


**Figure 10**. SEM micrograph of ZU3 as-tempered showing primary TaC particles and Ta oxide inclusions together with their EDX spectra.

Non-metallic inclusions are compounds that are embedded inside steel during manufacturing process. In the ZU series, compared to ZL3 (the alloy designed in the previous project KME 510), the number of these inclusions is higher. There are basically two different families of inclusions in the ZU alloys. The first group is oxides. As it is shown in Figure 11, these oxides are Ta oxides and aluminium oxides. The other family of inclusions in the ZU series is sulphides, namely MnS. Different types of inclusions tend to agglomerate and form big inclusion clusters. In Figure 11, a typical inclusion in ZU series is shown. Generally, a too high number density and a too large size of oxides and sulphides in steels have a negative contribution to the mechanical properties.



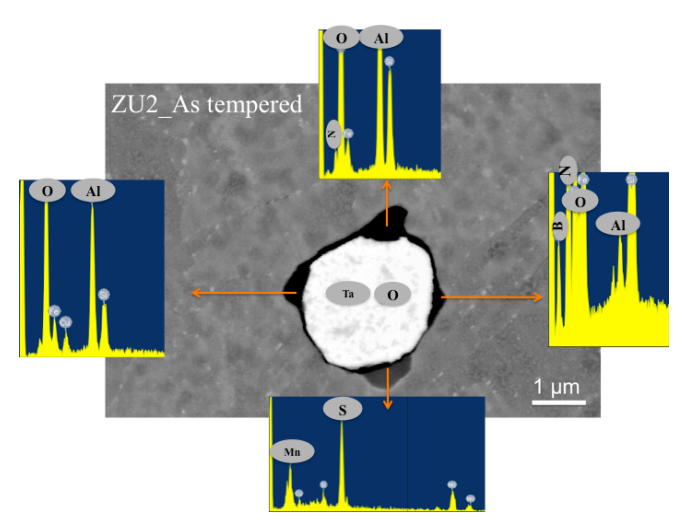


*Figure 11.* SEM micrograph showing different inclusions in ZU2 as-tempered steel. The same inclusions were found in ZU1 and ZU3.

We also made quantitative SEM measurements of the area fraction and size distribution of different primary particle families. The main findings are:

- Volume fraction of BN was highest in ZL3 and lowest in ZU3.
- ZU3 has the highest volume fraction of MX particles and ZU1 has the finest size distribution of MX particles.

For practical reasons, quantitative analysis of the particles is done in two series of measurements. First, all the particles bigger than 300 nm were analysed. Around 500 BN particles were analysed (approximately 2100 fields with the magnification of 2000 times). Figure 12 shows the BN area fraction for ZL3 and ZU1-3. As can be seen the BN area fraction in ZU3 is the lowest among other trial steels which shows a good trend in minimizing the unwanted BN particles.

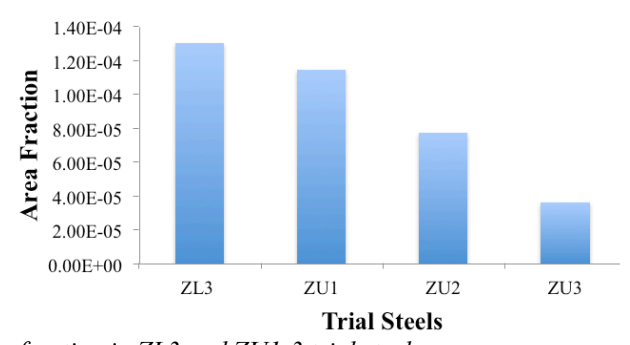


Figure 12. BN area fraction in ZL3 and ZU1-3 trial steels.

Figure 13 shows the mean size of BN particles. It is around 1.2  $\mu$ m in all steels except for ZU2, where the mean size was only 0.7  $\mu$ m. The relatively small size and very low area fraction of BN should not affect the mechanical properties (toughness, fatigue properties) to any large degree.



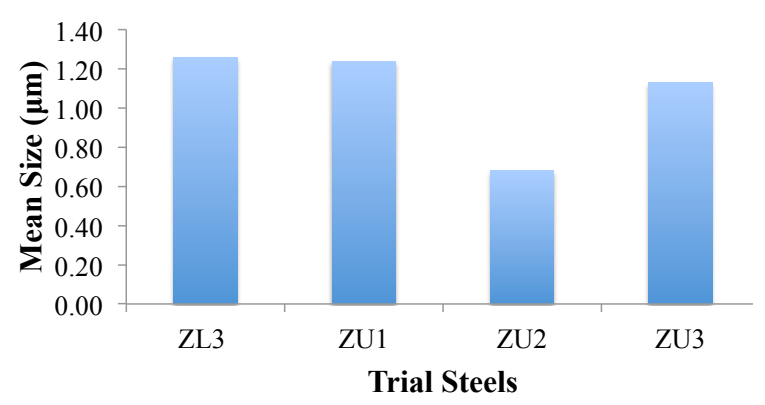


Figure 13. Mean size of BN particles in reference steel ZL3 and ZU1-3 trial steels.

In Figure 14, the size distribution of MX particles bigger than 300 nm is shown. MX is TaC in ZL3, ZU1, ZU3 and (Ta, Nb)(C, N) or TaC in ZU2.

In the second series of measurements, primary MX particles with sizes between 80 nm and 400 nm were analysed. These data are shown in Figure 15. Apparently ZU1 has the finest size distribution for primary MX particles and ZU3 has the highest volume fraction of MX particles probably due to high C and Ta content.

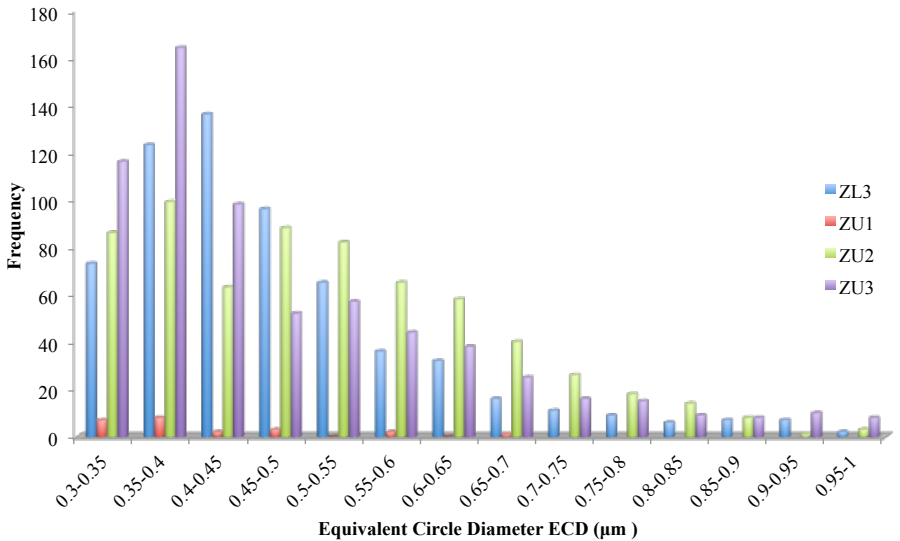


Figure 14. MX size distribution for particles bigger than 300 nm in ZL3 and ZU1-3.



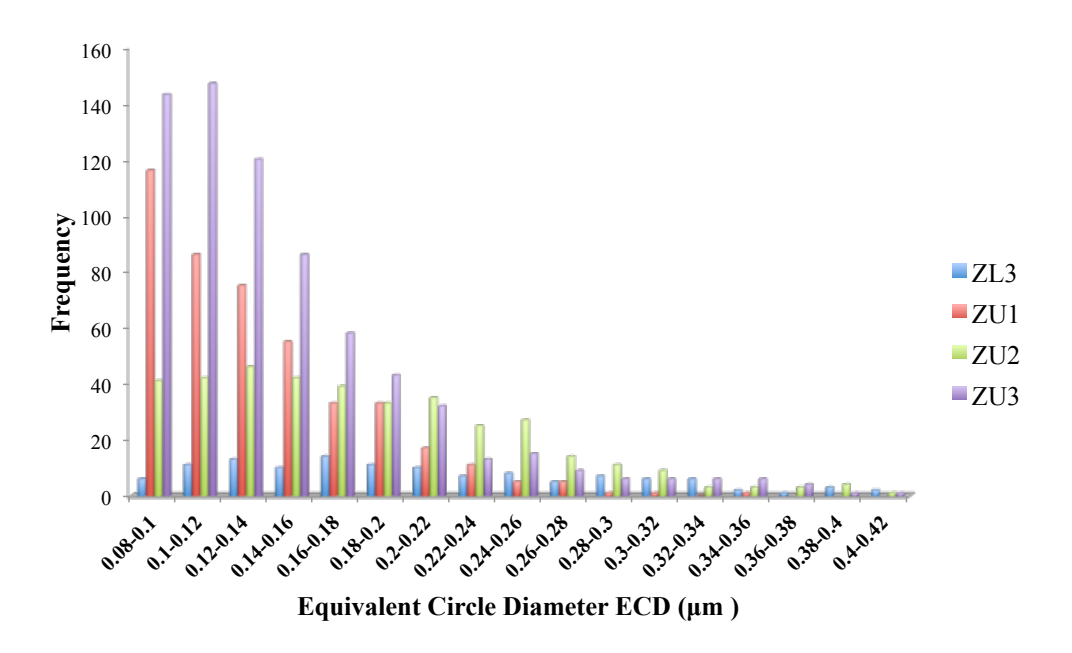


Figure 15. MX size distribution for particles bigger than 80 nm and smaller than 400 nm.

#### <u>δ-ferrite grains</u>

The formation of  $\delta$ -ferrite grains was observed in the ZU3 trail steel (Figure 7). This phase is believed to be detrimental and results in low toughness and ductility. However, a certain level of  $\delta$ -ferrite is acceptable for creep resistant steels, and the occurrence of a small amount of  $\delta$ -ferrite was actually expected in ZU3 in alloy designing.

#### Secondary precipitates

Figure 16 shows the distribution of Cu, C, Ta and TaN ions in one of the ZU1 APT specimens. Some Cu particles less than 10 nm in size were formed in ZU1 trial steel. Besides, three Ta(C,N) particles can be seen in the C, and Ta + TaN ion maps. The carbon and Cr content of these precipitates is approximately 30 at.% and 8 at.%, respectively (see Table 4). This high carbon content might make it harder for these precipitates to transform to Z-phase. Even though ZU1 contains less carbon compared to the reference material, ZL3, the formation of precipitates rich in C was observed.



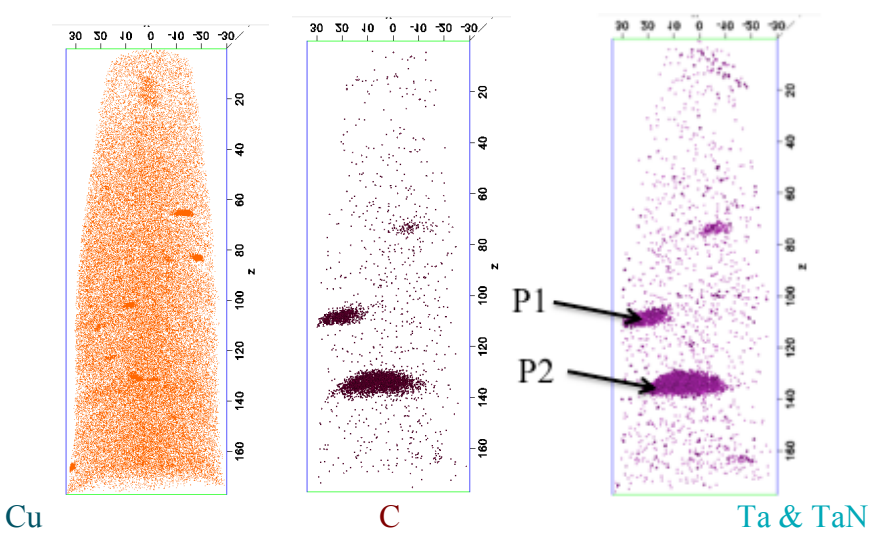


**Figure 16.** Reconstruction of an APT data set showing the distribution of Cu, C, and Ta + TaN ions in ZU1 trial steel. The arrows highlight two particles (P1 and P2) that contain C, Ta, and TaN. The chemical composition of P1 and P2 is provided in Table 4.

Table 4. Chemical composition of P1 and P2 precipitates highlighted in Figure 16.

	Ta	C	N	Cr	Fe	В	Co	W	V
Ta(C,N) (Middle)	36	31	17	8	2	2	0.3	1.6	0.7
Ta(C,N) (Lower)	45	26	12	7	6	1.6	0.3	0.1	0.25

In Figure 17, a precipitate of approximately 40 nm in size is shown in a reconstruction of an APT data set for ZU2 trial steel in the as-tempered condition. The chemical composition of this precipitate is provided in Table 5. Both Ta, and Nb have contributed to the formation of this carbonitride precipitates. Like alloy ZU1, which only contains Ta to form MX and further on Z-phase, combining both Ta and Nb also resulted in the formation of MX precipitates that are rich in C (23 at.%).

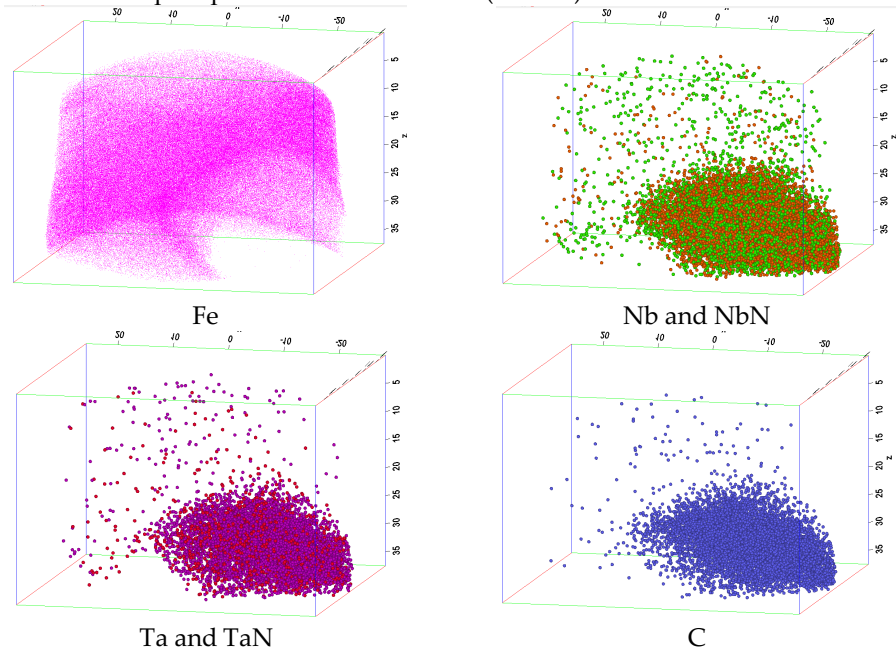


**Figure 17**. Reconstruction of an APT data set showing one (Ta,Nb)(C,N) precipitate. The chemical composition of this precipitate is provided in Table 7.



**Table 5.** Chemical composition of the (Ta,Nb)(C,N) precipitate shown in Figure 17.

	Ta	Nb	C	N	Cr	Fe	В	Co	W	V
(Ta,Nb)(C,N)	20	29	23	21	4.5	0.18	0.28	-	0.22	-

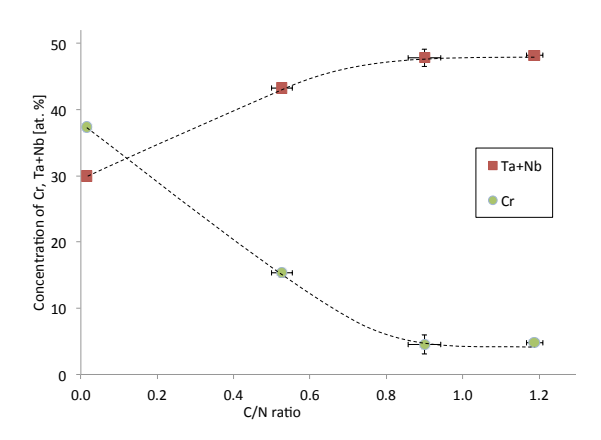


**Figure 18**. Concentration of Cr and Ta+Nb as a function of C/N ratio in carbonitrides and Z-phase precipitates in the trial steel. The dashed lines were drawn to guide the eye.

In ZU2 the secondary precipitates mainly contain Ta, Nb, and N and varying amounts of Cr, and C. The obtained results from the composition of different precipitates are summarized in Figure 18. The Cr content and the sum of the Nb and Ta content are plotted as a function of the C/N ratio. The particle with a C/N ratio almost equal to zero is a Z-phase particle, which contains only Ta, Nb, Cr, and N and trace amounts of C and Fe. Particles with high C/N ratio contain a small amount of Cr (~5%), and a high amount of Nb+Ta (~50%), which means that they are MX particles. In Figure 18 it is clearly shown that in precipitates with a low C content, the Cr content is high and the overall composition is close to the Z-phase composition. This trend indicates that the phase transformation from carbonitrides to Z-phase may require an extra step compared to the phase transformation from nitrides to Z-phase. In the latter case, nitrides transform to Z-phase by diffusion of Cr into nitrides, while in the former one, Cr in-diffusion and C out-diffusion need to be completed for a full transformation to Z-phase.

Figure 19 shows an EDX linescan across a Z-phase precipitate. It shows that the equilibrium composition of Z-phase contains more Nb than Ta, even if the ratio Nb/Ta is not as high as that found with APT. Both the TEM and APT results show that the composition of Z-phase with both Nb and Ta is quite close to the other previously reported compositions for Z-phase,  $Cr_{1+x}(Nb,Ta)_{1-x}N$ .



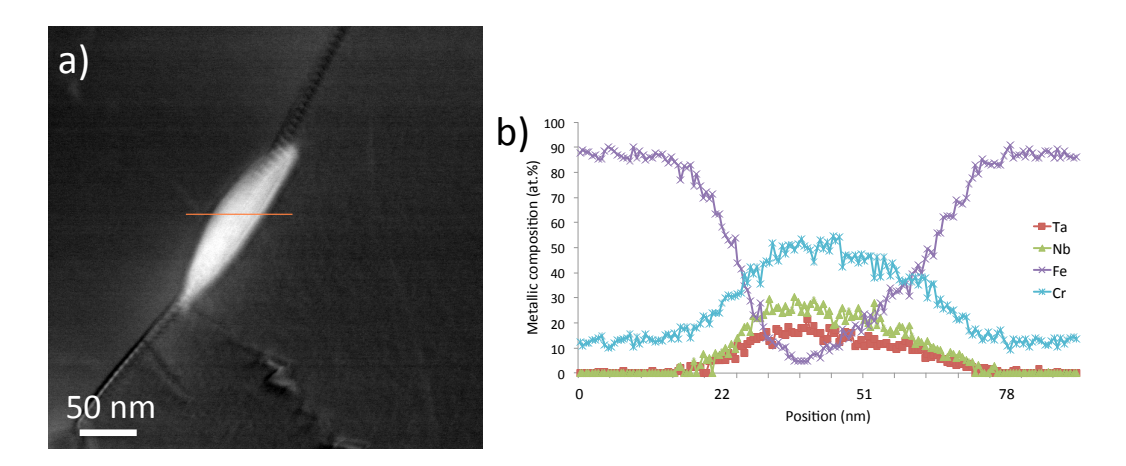


**Figure 19.** a) STEM micrograph of a Z-phase precipitate in the trial steel aged for 10,000 h at 650°C b) EDS linescan composition profile across the precipitate.

Figure 20 shows the distribution of different elements and a few nano-sized precipitates in one of the APT analyses. Ta(C,N) precipitates are shown by the Ta, TaN, and C ion maps. A Cr<sub>2</sub>N particle is shown by the Cr and CrN ion maps. As can be seen most of the particles are located on a boundary (the thread-like feature shown by the WN ion map).

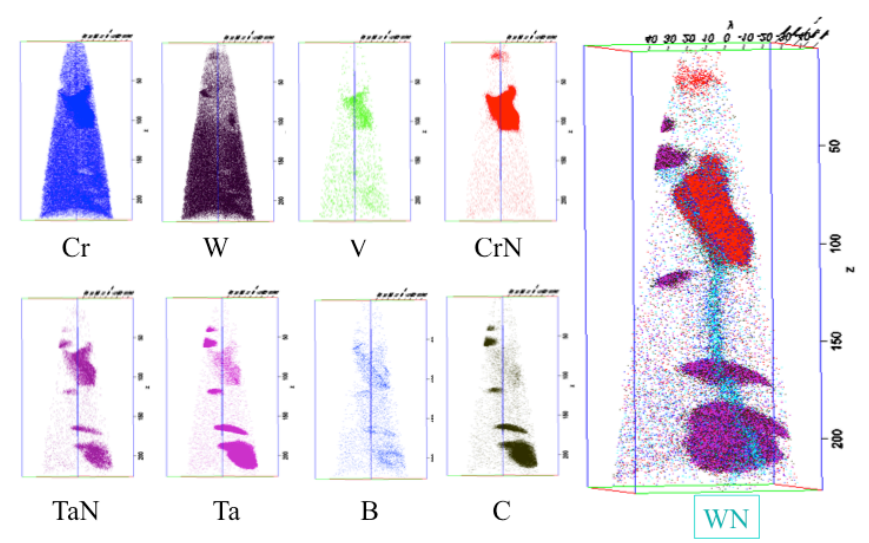


**Figure 20**. Reconstruction of an APT data set showing the distribution of different ions and a few nano-sized precipitates. Ta(C,N) precipitates are shown by the Ta, TaN, and C maps. A  $Cr_2N$  precipitate is shown by the  $Cr_2N$  map. A grain boundary is shown by the WN map.

As can be seen in the B map in Figure 20, most of the particles/matrix interfaces exhibit B ion segregation. Presence of B atoms at the interface between particle and matrix decreases the coarsening rate of the particles and this can result in better creep properties.



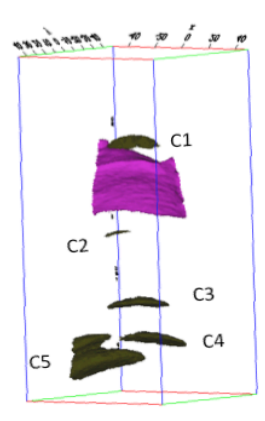


**Figure 21**. Iso-concentration surfaces showing different particles in ZU3 trial steel in the as-tempered condition. The black ones are Ta(C,N) particles, and the pink one is  $Cr_2N$ .

**Table 6**. Chemical composition of Ta(C,N) precipitates shown in Figure 21.

	Ta	C	N	Cr	Fe	В	Co	W	V
C1	50	40	8	1	0.26	0.27	-	-	-
C2	36	45	12	3	-	1.8	-	-	-
C3	44	42	11	2	-	0.17	-	-	0.12
C4	42	40	12	5	0.4	0.1	0.15	-	-
C5	42	36	12	6.3	1.5	0.2	-	-	0.19

Figure 21 shows the iso-concentration surfaces of different precipitates. The chemical composition of Ta(C,N) particles is provided in Table 6. The carbon content in ZU3 is much higher than ZU1 and ZU2, thus it is not surprising that C content in the MX precipitates is much higher (40% vs. 30%) compared to that in the MX particles in ZU1 and ZU2. The N and Cr content of MX particles formed in ZU3 trial steel are lower than those in MX particles in ZU1 and ZU2.

In order to study the effect of Mo addition on the formation of Laves phase in the testing alloy ZU3, we performed imaging analysis on backscattered micrographs taken in the SEM using the software ImageJ (Figure 22). Figure 23 shows the mean equivalent circle diameters  $\bar{d}$  as a function of aging time for steels ZU2 and ZU3 aged at 600 °C (blue), 650 °C (green) and 700 °C (red). Error bars are 95 % confidence intervals. Laves phase in the Mo and W containing trial steel ZU3 is smaller but shows a stronger tendency to coarsen than Laves phase in steel ZU2 that contains only W as a Laves phase forming element besides Fe.



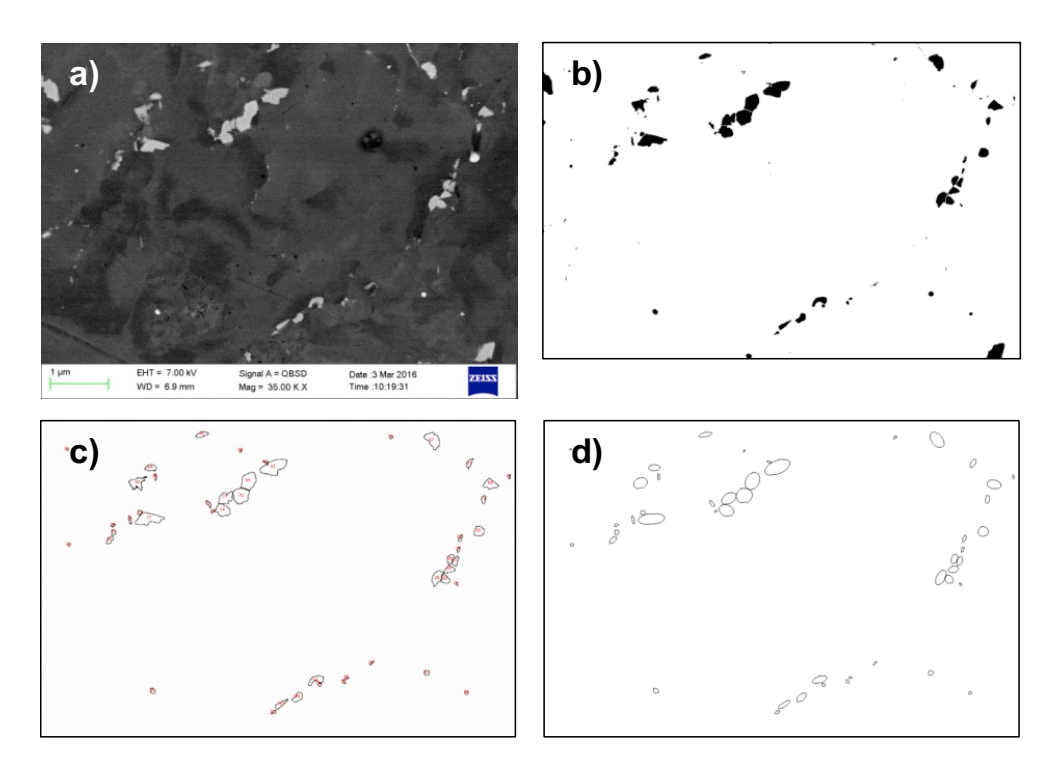
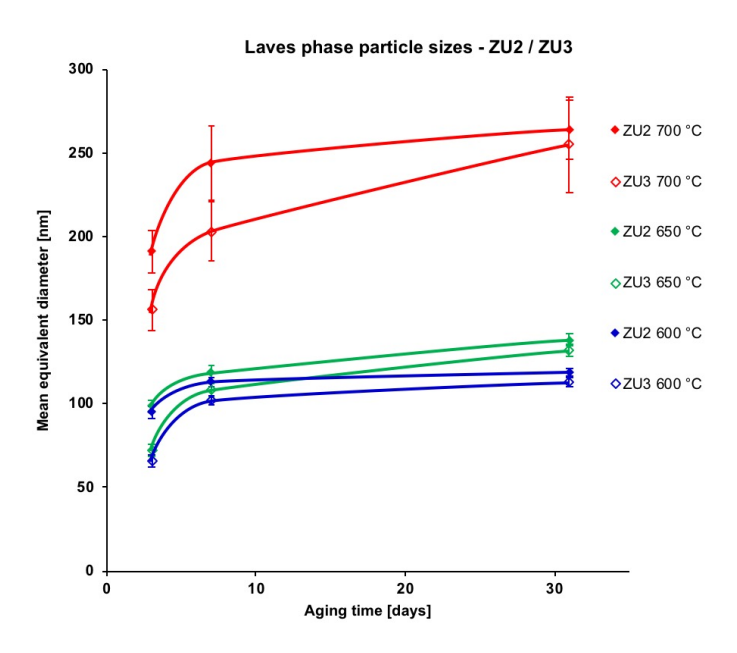


Figure 22. Image analysis with ImageJ: a) SEM micrograph; b) Micrograph after setting a threshold value (Laves phase is now black) c) Analysed particles using numbered outlines d) Analysed particles showing best fitting ellipses.



*Figure 23.* Mean equivalent circle diameters with 95 % confidence intervals of steels ZU2 and ZU3 versus aging time. Lines are trends of particle size evolution during aging.



# 4 Analysis of the results

#### 4.1 INCLUSIONS AND PRIMARY CARBONITRIDES

A small amount of BN inclusions was found in the trial steel. They partly consume beneficial elements of B and N. N was added to the alloy to form Z-phase. B is believed to control the coarsening behavior of secondary particles especially M<sub>23</sub>C<sub>6</sub>. BN formation decreases the effective N and B content in the alloy. In addition, extensive formation of BN inclusions can significantly impair the toughness of the steel. Consequently, the B+N content needs to be somewhat lower in future commercial Z-phase strengthened steels, to avoid BN formation.

Primary carbides of type TaC formed in ZU1 and ZU3, and carbonitrides of type (Ta, Nb)(C, N, B) formed in ZU2. These primary particles also consume Ta, Nb, and N, which were added to the steel mainly to form Z-phase. On the other hand, they have a positive effect on pinning the prior austenite grain boundaries and controlling the prior austenite grain growth. The prior austenite grain size was only 50 µm after austenitizing at 1100°C for 1 h, demonstrating that the primary carbonitrides were efficient in retarding grain growth. In case of Ta-based Z-phase strengthened steels, only primary TaC were observed. The combination of Nb and Ta apparently incorporates some N and B to the primary carbonitrides.

#### 4.2 SECONDARY PRECIPITATES

Z-phase based on Ta or Nb forms by diffusion of Cr into the TaN or NbN. The situation in the presence of C can be more complicated. C and N form carbonitrides in the steel and thus an extra step is required for a full transformation from carbonitrides to Z-phase, i.e. out-diffusion of C from carbonitrides. From the data obtained so far, two possible hypotheses regarding carbonitrides and Z-phase formation in the presence of a combination of Ta and Nb can be suggested:

First, MX carbonitrides are formed during the tempering process with a high C/N ratio and a Nb/Ta ratio of 1.6. Cr diffusion to the MX and C diffusion out from the MX result in phase transformation to Z-phase, which appears to have a higher Nb/Ta ratio than 1.6. This also requires the supply of additional Nb. It is worth mentioning that these precipitates are coarser compared to the pure Ta and Nb based Z-phase.

The second hypothesis is that two families of precipitates are formed during the tempering treatment; carbonitrides with a higher Nb/Ta ratio and carbonitrides with a lower Nb/Ta ratio. The former family of precipitates transforms faster to Z-phase compared to the latter one. This can potentially lead to co-presence of MX and Z-phase, which will eventually result in coarse Z-phase precipitates at the expense of small carbonitrides.



Comparing the creep data obtained from different Z-phase strengthened trial steels shows that the Ta-based Z-phase provides better creep properties than the Nb-based Z-phase. Creep data showed that the combination of Ta and Nb to form Z-phase did not improve the creep properties compared to the two former alloys. Ta resulted in formation of a fine distribution of Z-phase precipitates and subsequently good creep properties were achieved. The Z-phase precipitates were relatively coarser in the Ta plus Nb based Z-phase strengthened steel.

Laves phase in the Mo and W containing trial steel ZU3 is smaller but shows a stronger tendency to coarsen than Laves phase in steel ZU2 that contains only W as a Laves phase forming element besides Fe.



## 5 Conclusions

We succeeded in designing Z-phase strengthened steels with good general microstructure, i.e. with very small amount of detrimental delta-ferrite and primary particles. Delta-ferrite was only present in small amounts in one of the three testing alloys, which was predicted at the alloy design stage, meaning we can control the formation of delta-ferrite by designing the chemical composition. The volume fraction of the detrimental primary particle BN varied and followed closely with the B and N content, and the mean size is rather small. The common inclusions, i.e. alumina and manganese sulphide, together with tantalum oxide, were found in normal size and amount. These inclusions are unlikely to exert any negative influence on the creep resistance.

The primary MX precipitates had a small size (around  $0.1 \mu m$ ) and a dense distribution, which is beneficial for limiting the austenite grain growth during heat treatment.

To obtain very dense, finely distributed and slowly coarsening secondary precipitates of Z-phase is the primary means to achieve a good creep resistance. Within this project, firstly, we found that the alloy with both Nb and Ta exhibit poorer creep resistance than the alloys with only Ta. This is because adding both Nb and Ta to the testing alloy led to the formation of (Ta,Nb)(C,N); the transformation of (Ta,Nb)(C,N) to Z-phase was slower than that of Ta(C,N) to Z-phase. Secondly, rather bulky (Cr,Ta)2N exist in the alloys.

For the future, it is extremely important to study in detail how the ratio between C and N influences the phase transformations and thus creep properties of the Z-phase strengthened steels.



# 6 Goal fulfilment

The goals set for the project have been successfully fulfilled.

 design three new test steels with fine-tuned chemical composition, aiming for improved creep resistance compared to the ones that have been designed and investigated in the previous KME 510 project;

We designed and produced four new alloys: ZU1, ZU2, and ZU3; ZU1 showed better creep resistance compared to ZL3, which was designed in KME 510.

2. Optimize heat treatment conditions for test steels;

Austenitization at 1100°C, and two step tempering: 650°C for 4h + 750°C 2h gives good results.

3. Perform mechanical and creep testing on promising test steels with optimized heat treatment;

We have performed hardness testing (Vickers), impact toughness testing and long term creep testing on all the test steels (ZU1, ZU2, and ZU3).

4. Understand the sophisticated effects of carbon addition on the precipitation reaction sequences in the Z-phase strengthened steels;

Carbon addition delays the phase transformation into Z-phase. This is because carbon atoms participate into Ta(N,C), which then phase transform into Z-phase (CrTaN) by carbon diffusing out and Cr diffusing in.

5. Understand effects of small addition of B on the Z-phase strengthened steels;

Boron atoms segregate to different types of boundaries, and interfaces. There is ongoing work, in collaboration with the Technical University of Denmark, to reveal the nature of boron segregation.



# 7 Suggestions for future research work

We have proved that the new alloy design concept is feasible [12]. There are several important findings made by the research team: e.g. the benefit of using Ta-containing Z-phase (CrTaN) instead of Nb-containing one (CrNbN) or combined Ta- and Nb-containing one (Cr(Ta,Nb)N) to the creep strength of the steels, and the underlying mechanism [10,11]; the benefit of adding Cu to the impact toughness of the steels, and the underlying mechanism [13,14]; the complex but essential role of carbon in forming Z-phase [15,16].

In the future, it is of great importance to understand the essential role of the ratio between nitrogen and Ta, and nitrogen and carbon on the formation of Z-phase. These ratios may govern the pathway of forming Z-phase – from either MX (M = V, Nb, or Ta, X = C or N) or  $Cr_2N$  precipitates. Therefore, a fundamental understanding will provide us a potential strategy to control over the pathways of Z-phase precipitation in the new 12% Cr steels.

Additionally, it is important to systematically study the oxidation behaviours of the new 12% Cr steels, in comparison with 9% Cr steels, e.g. P92. For future application in power plants, the knowledge on oxidation is simply a must.

Last but not least, to select proper coatings to the 12% Cr steels, and study the interaction between the coating and the substrate steel are also of general interest for biomass power plants. 12% Cr steels with proper coatings allow higher efficiency and operational flexibility at a relatively low cost in biomass power plants. Therefore, study on coatings is necessary.



## 8 Literature references

- [1] International Energy Agency, http://www.iea.org, 2015.
- [2] International Energy Agency, France, 2016.
- [3] K. Maruyama, K. Sawada, J.-i. Koike, ISIJ International, 41 (2001) 641-653.
- [4] M. Taneike, F. Abe, K. Sawada, Nature, 424 (2003) 294-296.
- [5] T. Fujita, ISIJ International, 32 (1992) 175-181.
- [6] A.J. Sedriks, Chapter 10: Corrosion by hot gases and molten compounds, Corrosion of stainless steels, A Wiley-Interscience publication John Wiley & Sons, Inc., 1996.
- [7] T. Uehara, A. Toji, S. Komatsubara, T. Fujita, in: J. Lecomte-Beckers, M. Carton, F. Schubert, P.J. Ennis (Eds.) Materials for advanced power engineering, Forschungszentrum Jülich GmbH, Liege, Belgium, 2002, pp. 1311-1320.
- [8] A. Strang, V. Vodarek, Materials Science and Technology, 12 (1996) 552-556.
- [9] M. Svoboda, J. Bursik, I. Podstranska, A. Krouppa, V. Sklenicka, K.H. Mayer, in: J. Lecomte-Beckers, M. Carton, F. Schubert, P.J. Ennis (Eds.) Materials for advanced power engineering, Forschungszentrum Jülich GmbH, Liege, Belgium, 2002, pp. 1521-1530.
- [10] H. Danielsen, J. Hald, VGB Power Tech, (2009) 1-6.
- [11] W.O. Binder, Symposium on sigma-phase, Cleveland, OH, 1950, pp. 146.
- [12] F. Liu, M. Rashidi, L. Johansson, J. Hald, H.-O. Andrén, Scripta Materialia, Vol. 113, p. 93-96, (2016).
- [13] M. Rashidi, F. Liu, H.-O.Andrén, 10th Liège Conference on Materials for Advanced Power Engineering. (2014).
- [14] M. Rashidi, R. Lawitzki, H.-O. Andrén, F. Liu, EPRI 8th International Conference on Advances in Materials Technology for Future Power Plants, (2016).
- [15] F. Liu, M. Rashidi, J. Hald, L. Reißig, H.-O. Andrén, Materials Science Forum, Vol. 879, p. 1147-1152, (2016).
- [16] M. Rashidi, L. Johansson, H.-O. Andrén, F. Liu, Materials Science and Engineering A, Vol. 694, p. 57-65, (2017).
- [17] http://imagej.nih.gov/ij/index.html, 2011.



## 9 Publications

Results from the project have been presented in four articles in peer reviewed international journals, and four international conferences.

- A new 12% chromium steel strengthened by Z-phase precipitates
   F. Liu, M. Rashidi, L. Johansson, J. Hald, H.-O. Andrén
   Scripta Materialia, Vol. 113, 93-96, 2016.
- Microstructure of Z-phase strengthened martensitic steels: meeting the 650°C challenge F. Liu, M. Rashidi, J. Hald, L. Reißig, and H.-O. Andrén Materials Science Forum, Vol. 879, 1147-1152, 2016.
- Core-Shell Structure of Intermediate Precipitates in a Nb-Based Z-Phase Strengthened 12% Cr Steel
   M. Rashidi, H.-O. Andrén, F. Liu Microscopy and Microanalysis, Vol. 23, 360-365, 2017.
- Microstructure and mechanical properties of two Z-phase strengthened 12% Cr martensitic steels: the effects of Cu and C
   M. Rashidi, L. Johansson, H.-O. Andrén, F. Liu
   Materials Science and Engineering A, 694, 57-65, 2017.
- Microstructure characterization of two Z-phase strengthened 12% chromium steels
  M. Rashidi, F. Liu and H.-O.Andrén
  10th Liège Conference on Materials for Advanced Power Engineering. September 14th 17th,
  2014.
- Tantalum and niobium based Z-phase in a Z-phase strengthened 12% Cr steel
  M. Rashidi, R. Lawitzki, H.-O. Andrén, and F. Liu
  EPRI 8th International Conference on Advances in Material Technology for Fossil Power
  Plants, October 11 -14, 2016.
- On the non-equilibrium segregation of Boron in 9-12%Cr steels
   I. Fedorova, F. B. Grumsen, F. Liu, J. Hald
   4th International ECCC Creep & Fracture Conference, September 10-14, 2017, Düsseldorf, Germany.
- Role of copper on Laves phase morphology in 9-12%Cr steels
   H. K. Danielsen, F. Liu
   IOP Conference Series: Materials Science and Engineering, Volume 219. 38th Riso
   International Symposium on Materials Science, Riso, Denmark, 4-8 September 2017. IOP Conf. Ser.: Mater. Sci. Eng. 219, 012015



# 10 Appendices

#### 10.1 EXPERIMENTAL METHODS

#### 1. Materials preparation

The test steels were produced in 80 kg ingots by Vacuum Induction Melting (VIM) process. The ingots were hot rolled into 20 mm thick plates, and subsequently followed by different quality heat treatment conditions: austenitization, quenching, and tempering.

#### Mechanical testing

All mechanical testing were conducted according to corresponding European testing standard listed in Table A1.

Table A1. Standards used for mechanical testing.

Type of testing	Standard		
Hardness	EN ISO 6507-1:2005 (30 kg		
	load)		
Impact	EN ISO 148-1:2010		
Tensile testing at room	EN ISO 6892-1:2009		
temperature			
Tensile testing at elevated	EN ISO 6892-2:2011		
temperatures			
Interrupted and	EN ISO 204:2009		
uninterrupted creep rupture			
testing			

Interrupted creep rupture tests were carried out at 625°C with nominal stresses of 150, 125, 100 and 75 MPa, using specimens of approx. 5 mm in diameter and 30 mm in gauge length. Uninterrupted creep rupture tests were carried out at 650°C with nominal stresses of 120, 100 and 80 MPa, using specimens of approximately 7 mm in diameter and 50 mm in gauge length.

#### 3. Sample preparation for SEM

The SEM samples were prepared by mechanical polishing on a polishing machine: ground and polished until 1 micrometre diamond spray, and finishing with 0.25 micrometre colloidal SiO<sub>2</sub> suspension.

#### 4. Sample preparation for TEM

TEM specimens were prepared by the standard electropolishing method. The steels were first cut to  $\sim$ 0.25 mm thin slices using a low speed saw, and then mechanical polished down to  $\sim$ 0.05 mm. Then the polished thin slice was punched to 3 mm discs, followed by electropolishing in an electrolyte of 10% perchloric acid in methanol at -35 $^{\circ}$ C.



#### 5. Sample preparation for APT

The steels were cut into small rods ( $\sim 8 \times 0.25 \times 0.25 \text{ mm}^3$ ) by a low speed saw. The rods underwent a two-step electropolishing procedure in order to obtain APT samples with a final radius of less than 50 nm. First a thin neck was produced in 10% perchloric acid in methanol. Then fine polishing was made in a bath of 2% perchloric acid in 2-butoxyethanol until the lower part of the rod dropped off. All the APT samples were examined in a Leo Ultra 55 Field Emission Gun Scanning Electron Microscope (FEG-SEM) before being investigated in the atom probe.

#### 6. SEM

The prepared SEM samples were examined in a Leo Ultra 55 Field Emission Gun Scanning Electron Microscope (FEG-SEM). Chemical analysis was done by the Oxford Inca Energy Dispersive X-ray Spectrometry (EDX) system fitted to the SEM. The operation voltage was at 20 kV.

#### 7. TEM

A FEI-Titan 80 and a TECNAI (200 kV) equipped with an EDX were used to characterize microstructure of the Z-phase strengthened steels.

#### 8. Atom probe tomography

In order to analyse the chemical composition of the matrix as well as the small precipitates of the steels an Imago LEAP 3000X HR local electrode atom probe instrument was used. The sample temperature during analysis was in the range of 55-65K. For the Nb-containing steel, the pulsed voltage mode was used with a pulse fraction of 20%. To avoid premature specimen failure for Ta-containing steel pulsed laser mode was used, with a laser energy of 0.3 nJ. The acquired data were further analysed by using the IVAS<sup>TM</sup> software developed by Imago.

#### 9. Proxigram

In order to obtain accurate chemical information across certain interface, we used the socalled proxigram (proximity histogram), an embedded function in the APT reconstruction program. Here we explain how this function works. To get the chemical composition across an interface, we can take a volume, e.g. a cylinder, which includes the interface, which is often defined by the continuous surface with the same concentration for certain element, the so-called iso-concentration surface. Then we calculate the concentration data along the height. It is very important that the direction of the height of cylinder is perpendicular to the interface plane, in order to avoid smearing of the interface concentration. However, since the interfaces are usually irregular, it is often impossible to define just one volume, which covers the entire interface and simultaneously has the height perpendicular to the entire interface. What the proxigram algorithm does is to create a very small cylinder, make it move over the entire interface, while changing its position to ensure that it is perpendicular to the interfaces, calculate the concentration and finally integrate it over for the entire interface. In this way, a composition profile over the interfaces with much less smearing is obtained.



## 10. Image process and analysis

The image process software Image J [27] was used for analysing SEM secondary electron images. A threshold was set and applied for each SEM images in order to convert them to binary images for analysis. Information about precipitate number, size and area fraction was stored in a text file, which was then handled using Excel.



# Design a new generation of 12% chromium steels

Electricity generation from biomass will play an important role in the future. The main barriers to widespread use of biomass to generate electricity are cost and low energy efficiency, which is, in turn, limited by the materials.

The proposed project aims to address the material challenges by using a new alloy design concept for 12% Cr steels – Z-phase strengthening. This is the only possible solution today to achieve both good creep and oxidation resistance for 12% Cr steels at 650°C.

Based on our success in proving the novel concept of using Z-phase to strengthen 12% Cr steels from the previous KME project (KME-510), we continued our work on this new generation of martensitic steels. Within the frame of this project, we designed three new alloys. The aim was to understand the important factors that influence Z-phase formation, and thus aid the development Z-phase strengthened steels with high creep resistance. Firstly, we showed that Z-phase strengthened steels containing both Nb and Ta yield poorer creep strength compared to those containing only Ta. Secondly, a two-step tempering heat treatment procedure was optimized for all three test steels. Thirdly, we found carbon concentration was extremely important in the process of phase transformation to Z-phase; a high carbon concentration delayed the phase transformation. Therefore, we conclude a fine tune of the carbon concentration is essential in this type of steels. Finally, we found boron atoms segregated to prior austenite boundaries, lath boundaries, and the interface between Z-phase and steel matrix. The segregation likely plays an important role in lowering the interface energy, thus improving creep resistance.

Energiforsk is the Swedish Energy Research Centre – an industrially owned body dedicated to meeting the common energy challenges faced by industries, authorities and society. Our vision is to be hub of Swedish energy research and our mission is to make the world of energy smarter. www.energiforsk.se

